Chemistry–A European Journal
Minireview
doi.org/10.1002/chem.202004563
Chemistry Europe
European Chemical Societies Publishing

Bond Activation

Boron–Ligand Cooperation: The Concept and Applications

Max Hasenbeck and Urs Gellrich*[a]

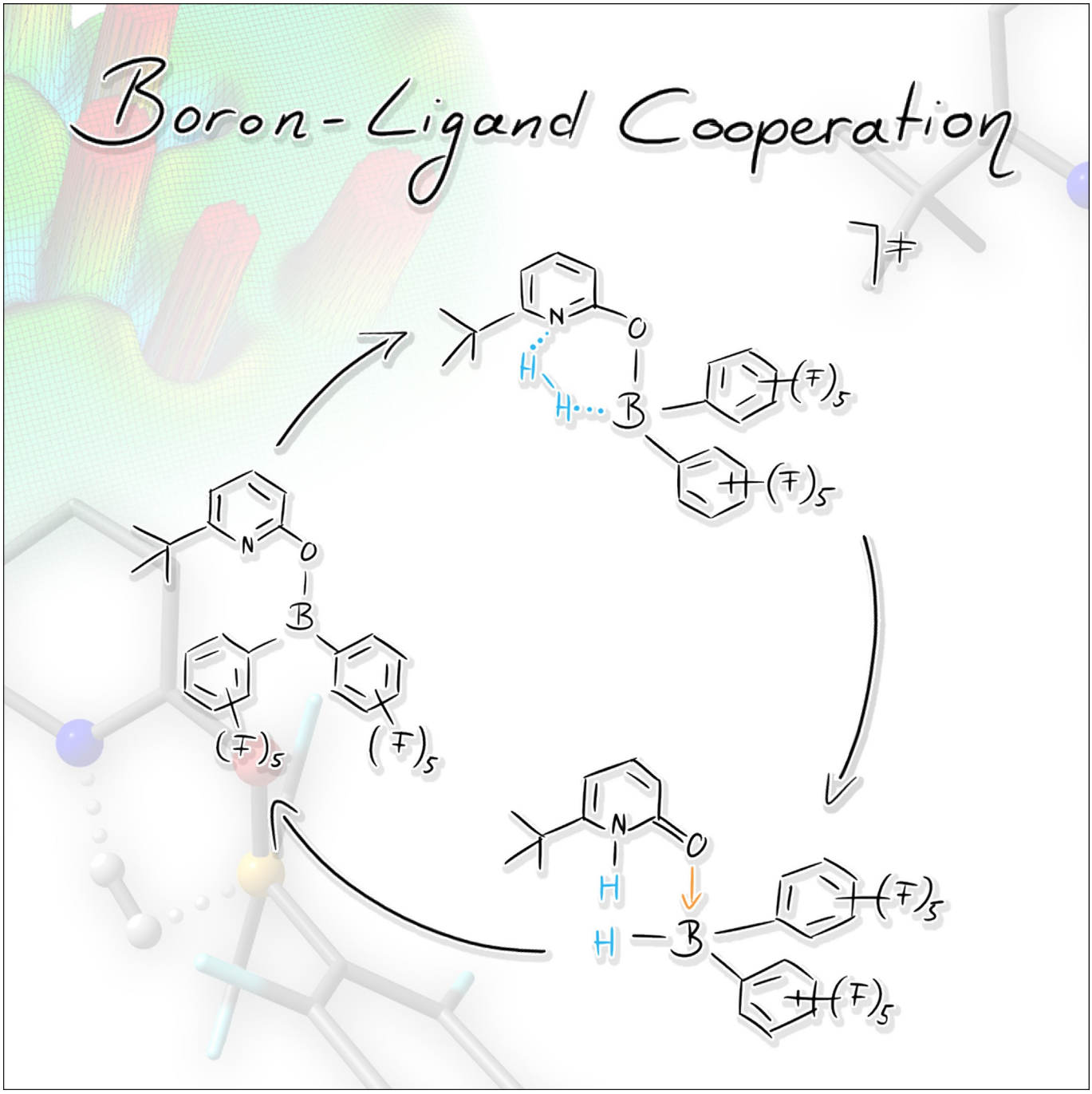

Abstract: The term boron–ligand cooperation was introduced to describe a specific mode of action by which certain metal-free systems activate chemical bonds. The main characteristic of this mode of action is that one covalently bound substituent at the boron is actively involved in the bond activation process and changes to a datively bound ligand in the course of the bond activation. Within this review, how the term boron–ligand cooperation evolved is reflected on and examples of bond activation by boron–ligand cooperation are discussed. It is furthermore shown that systems that operate via boron–ligand cooperation can complement the reactivity of classic intramolecular frustrated Lewis pairs and applications of this new concept for metal-free catalysis are summarized.

Introduction

The concept of boron–ligand cooperation was coined to describe a specific mode of bond activation by boranes that is reminiscent of the concept of metal–ligand cooperation. However, these boranes can also be described as a specific class of intramolecular frustrated Lewis pairs (FLPs). We, therefore, commence this review with a brief reflection on metal–ligand cooperation and frustrated Lewis pairs.

Metal–ligand cooperation

Metal–ligand cooperation (MLC) has emerged as a powerful tool for bond activation and catalysis in the last decades. Whereas classic transition-metal complexes activate chemical bonds by an oxidative addition at the metal center, MLC denotes a situation where one of the ligands bound to the metal center is actively involved in the bond activation process. Prime examples for bond activation by MLC are the hydrogen activation by Noyori's ruthenium catalyst **1** and by the ruthenium pincer complex **3** introduced by David Milstein and coworkers.[1,2] In the course of the hydrogen activation by the Noyori system, the amide substituent is involved in the H_2 activation. Hydrogen activation by the Milstein system is accompanied by the transfer of a proton to the benzylic position of the dearomatized pincer ligand, leading to a re-aromatization of the pyridine ring (Scheme 1).

In their comprehensive review on MLC from 2015,[3] Khusnutdinova and Milstein gave three criteria for MLC that read as:

"1) Both the metal and the ligand participate in the bond cleavage or bond formation steps;

2) Both the metal and the ligand are chemically modified during bond activation.

3) The coordination mode of the cooperative ligand undergoes significant changes in the first coordination sphere as a result of bond activation."

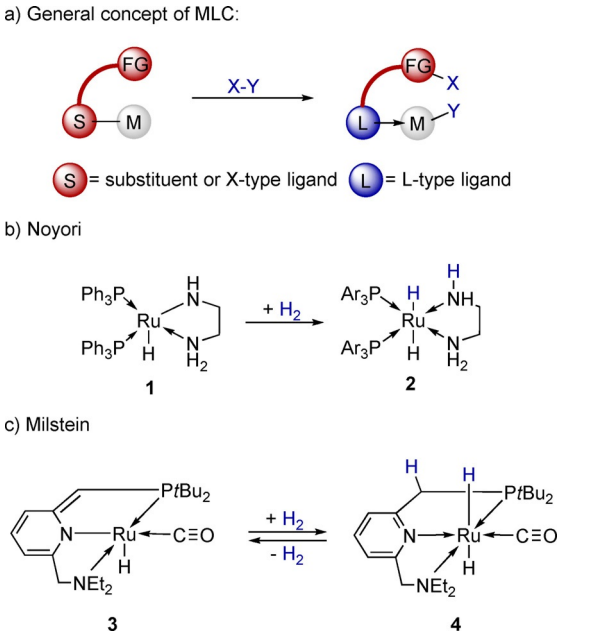

Scheme 1. The concept and examples of metal–ligand cooperation. (a) The concept of metal–ligand cooperation according to the criteria defined by Khusnutdinova and Milstein. (b) Hydrogen activation by Noyori's catalyst. (c) Reversible hydrogen activation by Milstein's pyridine-based pincer complex through an aromatization/de-aromatization sequence.

In the context of this review, it is important to emphasize the third criterion, which stipulates that the "*coordination mode of the cooperative ligand undergoes significant changes*" during bond activation. An analysis of the examples given in the review by Khusnutdinova and Milstein reveals that this change in the coordination mode can usually be described as the transition of a covalently bound substituent to a datively bound ligand. For example, the amide substituent in the Noyori system becomes a datively bound amine ligand during the bond activation. The re-aromatization that is observed upon bond activation by the Milstein pincer systems leads to the regeneration of a datively bound pyridine ligand, which was before bond activation better described as an enamide substituent. As a consequence of this change in the coordination sphere, the formal oxidation state of the ruthenium does not change. We note that inorganic chemists might prefer to describe this change in the coordination mode as the transi-

[a] *M. Hasenbeck, Dr. U. Gellrich*
Institut für Organische Chemie, Justus-Liebig-Universität Gießen
Heinrich-Buff-Ring-17, 35392 Gießen (Germany)
E-mail: urs.gellrich@org.chemie.uni-giessen.de
The ORCID identification number(s) for the author(s) of this article can be found under: https://doi.org/10.1002/chem.202004563.

tion of an X-type ligand to an L-type ligand.[4] However, we use the term "covalently bound substituent" here as equivalent to the notation X-type ligand to establish an analogy to transition-metal-free systems.

Frustrated Lewis pairs

The term frustrated Lewis pairs (FLPs) describes combinations of sterically encumbered Lewis bases and Lewis acids that are able to activate strong chemical bonds.[5,6] Classic examples for intramolecular FLPs are the covalently linked phosphine–borane pairs **5** and **7** developed by the groups of Stephan and Erker (Scheme 2).[5a,b] The hydrogen activation by these intramolecular FLPs leads to the formation of borohydrides (**6** and **8**). Numerous metal-free catalytic reactions that are based on the FLP concept have been developed in recent years.[6]

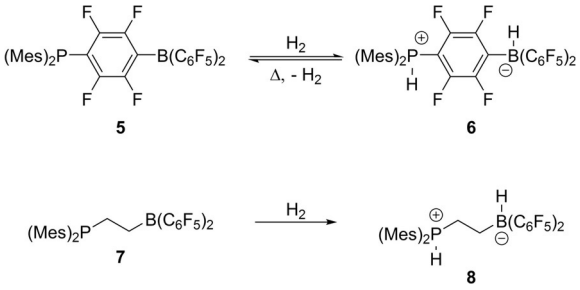

Scheme 2. Hydrogen activation by the intramolecular FLPs **5** and **7**, which leads to the formation of the borohydrides **6** and **8**.

Boron–ligand cooperation: The concept

We and others recently reported bond activation by a specific class of intramolecular FLPs in which bond activation leads to a reorganization of π-electron density within the cooperative substituent. Furthermore, bond activation is associated with a transition of the involved substituent to a datively bound ligand (Scheme 3 a). Thus, in contrast to classic FLPs, bond activation does not lead to a borate salt, but rather a borane complex. We note that the reorganization of π-electron density and the concomitant change in coordination mode of the cooperative substituent are reminiscent of hydrogen activation by Milstein's established pyridine-based pincer complexes (Scheme 3 b).[2,3] In analogy, we proposed the term boron–ligand cooperation (BLC) to describe the bond activation by these specific FLPs.

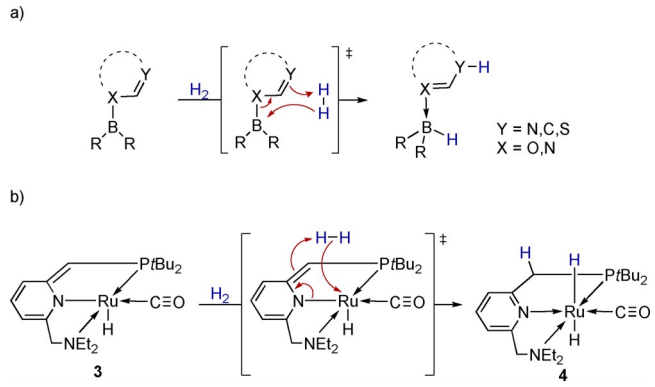

Scheme 3. Hydrogen activation by a specific class of intramolecular FLPs, which leads to a change in the bonding mode of the cooperative substituent (a) and the analogy to hydrogen activation by the pincer complex **3** (b).

Thus, the BLC concept emphasizes a change in the valence sphere of the borane as a result of the bond activation. However, the systems that operate through BLC can in their reactive state before bond activation be classified as intramolecular FLPs. The three concepts of MLC, FLPs, and BLC have in common that the bond activation involves two active sites with Lewis basic and Lewis acidic character. These similarities were noted in recent reviews by Greb and Slootweg.[7] Within the second part of this review, we will discuss examples of bond activation by BLC with a special emphasis on changes in the bonding between the substituent involved in the bond activation and the borane. In the third part, we will discuss how the novel reactivity based on BLC can complement the reactivity of FLPs and show how the BLC concept can lead to new applications for transition-metal-free catalysis.

Bond Activation by Boron–Ligand Cooperation

In the following, we will discuss examples of bond activation that fulfill the criteria for BLC formally. We will focus on the question of whether experimental and computational data further support that the transition of a covalently bound substituent to a datively bound ligand is a real chemical event.

Max Hasenbeck studied chemistry at the universities of Cologne and Düsseldorf in Germany. For his master's thesis, he worked on the computational investigation of reaction mechanisms under the supervision of Dr. Martin Breugst. After receiving his M.Sc. in 2017, he joined the group of Dr. Urs Gellrich at the Justus Liebig University Giessen for his doctoral studies working on the concept of boron–ligand cooperation and its application for catalysis.

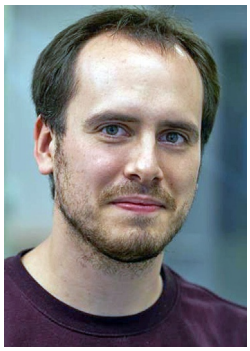

Urs Gellrich studied chemistry at the University of Freiburg in Germany where he obtained his doctorate in 2013 for his work on supramolecular ligands under the guidance of Prof. Bernhard Breit. He then joined the group of Prof. David Milstein at the Weizmann Institute of Science as a postdoctoral researcher. In 2017, Urs started his independent career as a Liebig Fellow of the FCI at the Justus Liebig University Giessen where he is currently Emmy Noether Group Leader. His research focuses on the in silico design of novel metal-free systems for bond activation and catalysis.

Early examples of boron–ligand cooperation

In 2010, Tamm and co-workers reported the H_2 activation by the pyrazolylborane **9**, which the authors described as a bifunctional FLP (Scheme 4).[8] The authors reported the product **10** of the hydrogen activation as zwitterionic pyrazolium–borate. However, **10** can also be described as a pyrazol borane complex. The elongation of the N–B bond from 1.4281(16) Å in **9** to 1.5794(13) Å in **10**, determined by single-crystal (SC)XRD, does support this description.

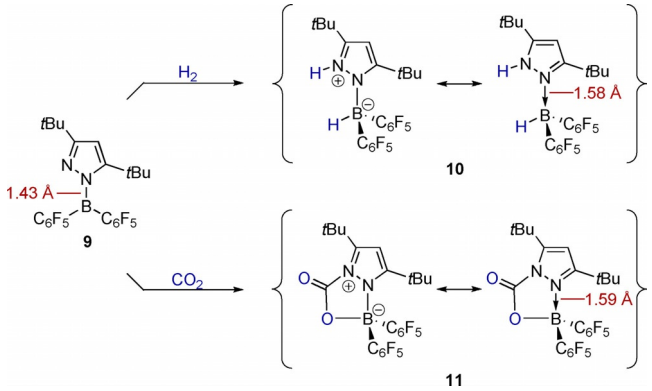

Scheme 4. Hydrogen and CO_2 activation by the pyrazolylborane **9** and the possible description of the products as zwitterionic pyrazolium–borate or as pyrazol borane complex.

A similar bond elongation is observed upon CO_2 activation by **9**, which yields **11**.[9] An alternative interpretation is that the N–B π-bonding in **9** is lost upon hydrogen activation, resulting in an elongation of this bond. However, the reported SCXRD structures further reveal that upon hydrogen activation the N1–C3 is shortened by 0.05 Å whereas the N2–C1 is elongated by 0.03 Å (Scheme 5). This change in the bond lengths, indicating a reorganization of π-electron density within the heterocycle upon hydrogen activation, is better described when **10** is depicted as a pyrazole borane complex.

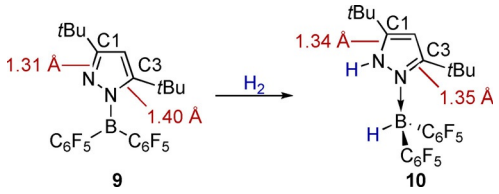

Scheme 5. Changes in the bond lengths of the heterocycle upon hydrogen activation by **9** derived from SCXRD structures.

A computational examination of boron–ligand cooperation

To mimic the reactivity of Milstein's ruthenium pyridine pincer complex by metal-free systems, Wang, Schleyer, and colleagues investigated the activation of dihydrogen by model compound **12** (Scheme 6).[10] From their computations, the authors concluded that hydrogen activation by **12** yielding **13** is kinetically feasible but that the reverse reaction is not possible. The computed nucleus independent chemical shifts (NICS(0))[11] further reveal an aromaticity gain upon hydrogen activation by **12**, which is diagnostic for the formation of a datively bound pyridine ligand.

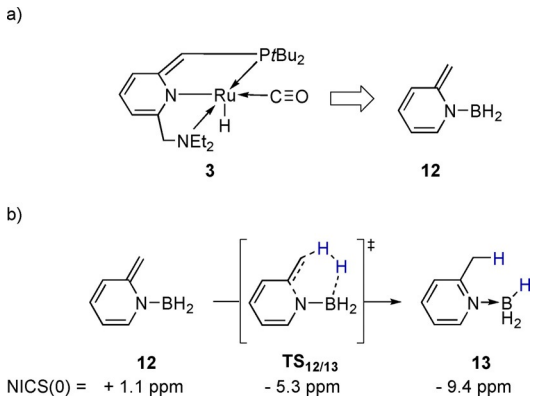

Scheme 6. The model system **12**, designed to mimic the reactivity of Milstein's ruthenium pincer complex and the re-aromatization of **12** upon hydrogen activation, which is exemplified by the computed NICS values.

Although the authors did not use the term BLC, this computational study named MLC as a design principle for bond activation by a borane.

Boron–ligand cooperation by re-aromatization of a pyridine–borane complex

Inspired by the computational work by Schleyer and Wang, Milstein and co-workers attempted to realize bond activation by a dearomatized pyridine borane experimentally.[12] Therefore, the amino-borane pyridine complex **14** was synthesized (Scheme 7). Upon moderate heating, hydrogen liberation from **14** and formation of the dearomatized aminoborane **15** was observed.

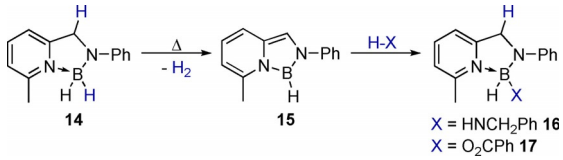

Scheme 7. Hydrogen liberation from **14** at elevated temperatures leads to de-aromatization of the pyridine ring. The reaction with benzylamine or benzoic acid results in re-aromatization of the pyridine ring.

As indicated by the ^{1}H NMR chemical shifts of **14** and **15** and the computed NICS values, the de-aromatization event is in this case better described as a shift of the aromaticity from the pyridine ring in **14** to the five-membered boracycle in **15**. The reaction of **14** with benzylamine or benzoic acid leads to N–H activation and O–H cleavage and formation of **16** and **17**, respectively. In both cases, the re-aromatization of the pyridine ring shows that the bond activation was accompanied by the change of the N–B bond from a covalent bond in **15** to a

dative bond in the pyridine amino-borane complexes **16** and **17**. To describe the reactivity of **15**, the term boron–ligand cooperation was introduced.

Boron–ligand cooperation by a pyridonate borane

In 2018, we reported reversible H_2 activation by the pyridonate borane complex **18** (Scheme 8).[13] The closed-form of the pyridonate borane **18** is in equilibrium with the open form **18′**, which can be regarded as an intramolecular FLP. Hydrogen activation by **18′** yields **19**. The hydrogen activation is reversible. Upon heating to 60 °C, **19** liberates dihydrogen and **18** is regenerated.

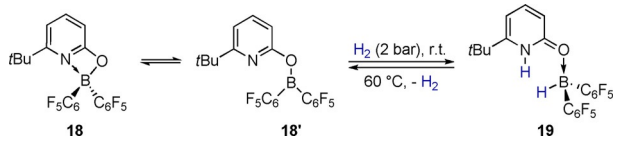

Scheme 8. Reversible hydrogen activation by **18′**, leading to the formation of the pyridone borane complex **19**.

We became interested if **19** is better described as zwitterionic borate or as a pyridone borane complex. A comparison of the computed structures of **18′** and **19** reveals an elongation of the O–B bond by 0.2 Å (Scheme 9). Furthermore, the C–O is shortened in course of the bond activation to 1.27 Å, a value that is typical for a C=O double bond. This indicates that the heterocycle in **19** is present as pyridone. In agreement with this interpretation, the C=O stretching vibration of **19** at 1643 cm^{-1} is similar to that observed for the "fixed" pyridone tautomer 1-methyl-2-pyridone.[14] The reduced aromaticity of **19** compared with **18**, deduced from the computed NICS values, is further indicative of the formation of a pyridone.[15]

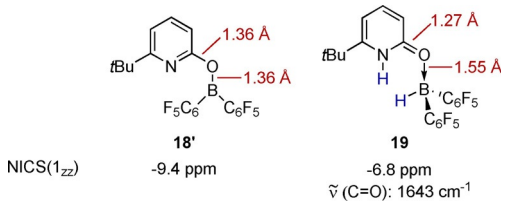

Scheme 9. Computed bond lengths and NICS values for **18′** and **19**. The description of the pyridone borane complex is further supported by the experimentally determined IR stretching vibration of **19**.

The disappearance of the covalent B–O upon dihydrogen activation of **18′** to **19** is furthermore supported by the analysis of the Laplacian of the electron density (Figure 1). For covalent bonds, the Laplacian of the electron density should show a minimum along the bond axis.[16] In the case of pyridonate borane **18′**, this is clearly visible ("blue valley", Figure 1, left side). This is not the case for pyridone borane **19** (Figure 1, right side), indicating a closed-shell interaction between O and B. An EDA-NOCV analysis further supports the change in the bonding mode of the pyridonate substituent upon hydrogen activation.[17]

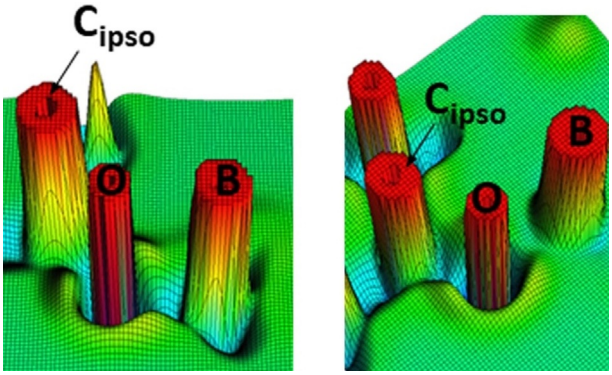

Figure 1. Analysis of the Laplacian of the electron density computed at PBE0(D3BJ)/def2-TZVP.[18] Left: pyridonate borane **18′**; right: pyridone borane complex **19**.

Boron–ligand cooperation as a concept for metal-free catalysis

The IUPAC definition of a dative bond states that "The distinctive feature of dative bonds is that their minimum-energy rupture in the gas phase or in inert solvent follows the heterolytic bond cleavage path".[19] To substantiate the presence of a dative bond in **19**, we probed the heterolytic dissociation in a pyridone and a borane (Scheme 10). As the equilibrium lies far on the side of the pyridone borane complex, there is no possibility to obtain direct spectroscopic evidence for such a dissociation. Therefore, we investigated if **19** is able to effect hydroboration, as hydroboration requires the presence of a trivalent borane.[20] Indeed, when **18′** was reacted under an H_2 atmosphere with styrene, the formation of the pyridone alkylborane **20** was observed (Scheme 10).

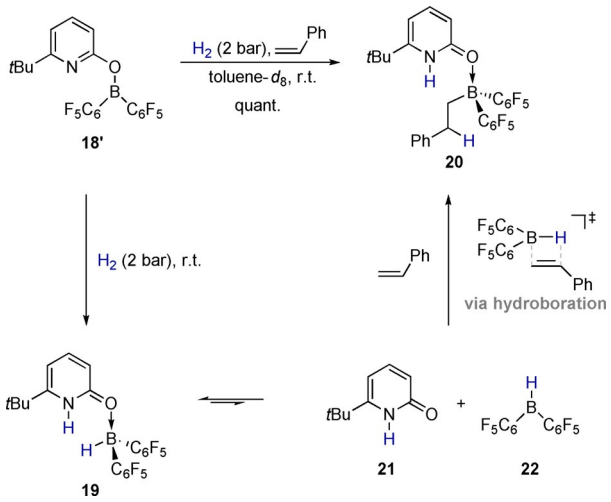

Scheme 10. Formation of the alkylborane **20**, which shows that the pyridone borane complex **19** formed upon H_2 activation by **18′** undergoes a heterolytic dissociation to pyridone **21** and Piers borane **22**.

Thus, the change of the B–O from a covalent bond to a dative bond during H_2 activation provides access to borane reactivity. Classic intramolecular FLPs rather show borohydride reactivity. In this regard, the concept of BLC complements the reactivity of classic FLPs.

Semi-hydrogenation of alkynes

Repo and co-workers showed that alkenyl borate complexes are prone to undergo intramolecular protodeborylations in the presence of protic substituents.[21] We, therefore, envisioned that a pyridone alkenylborane complex, formed analogously to **20** upon hydroboration of an alkyne, could undergo a protodeborylation yielding a *cis* alkene. This would enable the usage of **18′** as a potential hydrogenation catalyst in a sequence of H_2 activation, hydroboration, and protodeborylation. Using this strategy, several internal alkynes were hydrogenated in moderate to excellent yields under mild hydrogen pressure to the corresponding (*Z*)-alkenes (Scheme 11).[20,22]

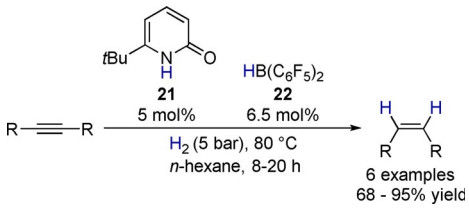

Scheme 11. *Semi*-hydrogenation of internal alkynes to the corresponding (*Z*)-alkenes.

Extended reaction times lead to the isomerization of the (*Z*)-alkenes to the corresponding (*E*)-alkenes for some substrates. We attributed this isomerization to the reversible hydroboration of alkenes by the Piers borane, which was reported earlier by the Du group.[22a] The reaction mechanism of the hydrogenation was investigated experimentally and computationally (Scheme 12). After hydrogen activation by the pyridonate borane **18′**, the resulting pyridone borane complex **19** dissociates into the pyridone **21** and Piers borane **22**. This endergonic reaction is rendered thermodynamically more favorable by the complexation of the pyridone **21** with the pyridonate borane **18′**, yielding the bispyridone complex **23**.[13,23] After hydroboration of the alkyne by Piers borane **22**, the resulting alkenylborane **24** has to re-coordinate to the pyridone **21** to undergo protonolysis. Therefore, the bispyridone complex **23** has to dissociate again into the pyridonate borane **18′** and the pyridone **21**. The latter coordinates to alkenylborane **24**, yielding the alkenylborane pyridone complex **25**. Protodeborylation liberates the (*Z*)-alkene and regenerates the catalyst **18′**.

The bispyridone complex **23** and the alkenylborane **24** were identified as the resting state of the catalytic transformation by NMR spectroscopy, whereas computations identified the protodeborylation as the turnover-determining transition state (TDTS). For 2-butyne as a model substrate, the computed kinetic barrier or *energetic span* of the catalytic cycle is 22.6 kcal

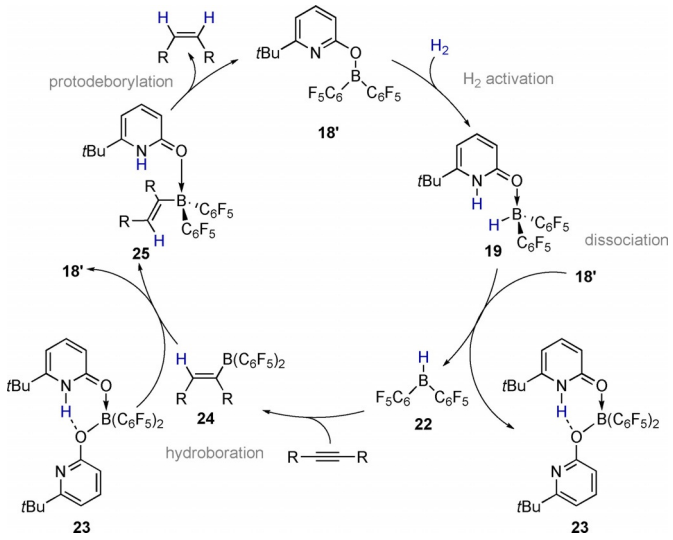

Scheme 12. Catalytic cycle of the *semi*-hydrogenation of internal alkynes to the corresponding (*Z*)-alkenes.

mol^{-1}, which is in good agreement with the experimental reaction conditions (Scheme 13).[24]

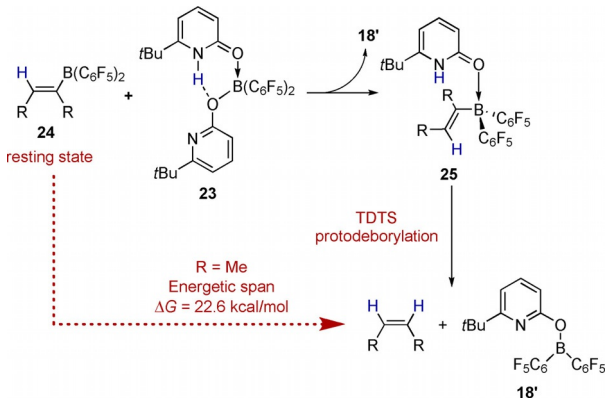

Scheme 13. Protoborylation of the alkenylborane and the computed energetic span of the catalytic cycle at revDSD-PBEP86-D4/def2-QZVPP//PBEh-3c.[25] The SMD model for *n*-hexane was used to account implicitly for solvent effects.[26]

Furthermore, several terminal alkynes could be hydrogenated in moderate to good yields although a higher catalyst loading had to be used (Scheme 14a). This is the first example of an FLP catalyst which is able to hydrogenate terminal alkynes. Other FLPs are deactivated by terminal alkynes because of an irreversible deprotonative borylation.[27] Although pyridonate borane **18′** reacts with terminal alkynes in such a deprotonative borylation, a competition experiment revealed that the C_{sp}–H cleavage is reversible, thus enabling the hydrogenation pathway (Scheme 14b).

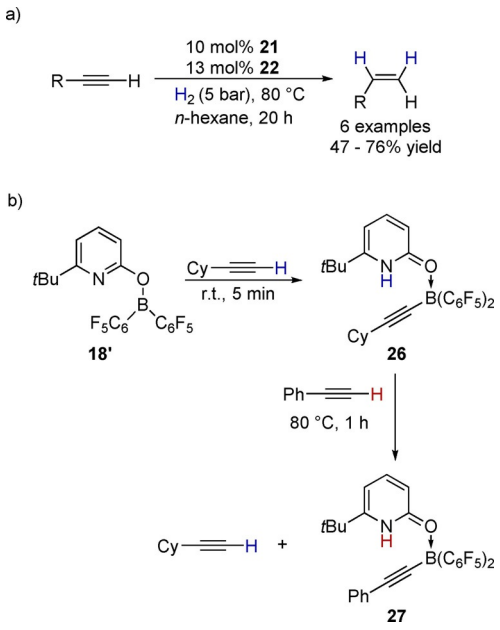

Scheme 14. (a) Scope of the *semi*-hydrogenation of terminal alkynes, (b) competition experiment of the C_{sp}–H cleavage of terminal alkynes by **18′**.

Gem-dimerization of terminal alkynes

The ability of **18′** to cleave the C_{sp}–H bond of terminal alkynes was used to develop a catalytic protocol for the first metal-free *gem*-dimerization of terminal alkynes.[28] By heating a reaction mixture of a terminal alkyne with 20 mol% of the pyridonate borane **18′**, several alkynes were dimerized to the respective enynes with exclusive *gem*-regioselectivity (Scheme 15). The active catalyst was formed *in situ* by dehydrogenation of **19**.

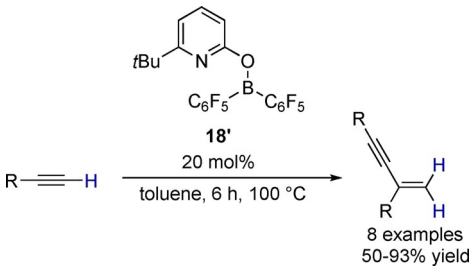

Scheme 15. *Gem*-dimerization of terminal alkynes by using pyridonate borane **18′** as the catalyst.

Mechanistic investigations reveal that for the observed reactivity, the change in the B–O bonding from a covalent to a dative bond upon C_{sp}–H activation of the terminal alkyne by the pyridonate borane **18′** is essential (Scheme 16). This change in the bond mode enables the dissociation of the pyridone alkynylborane complex **28** in the pyridone **21** and the trivalent alkynylborane **29**, which undergoes an 1,2-carboboration reaction with another equivalent of the terminal alkyne.[29] The resulting enynylborane **30** re-coordinates to the pyridone **21**, forming **31**. After protodeborylation, the *gem*-dimer is released and the catalyst **18′** is regenerated. Computations and experiments showed that the alkynylborane pyridone complex **28** is the resting state whereas the 1,2-carboboration is the TDTS of the reaction. The *energetic span* of the reaction for propyne as a model substrate was computed to be 25.0 kcal mol^{-1}.

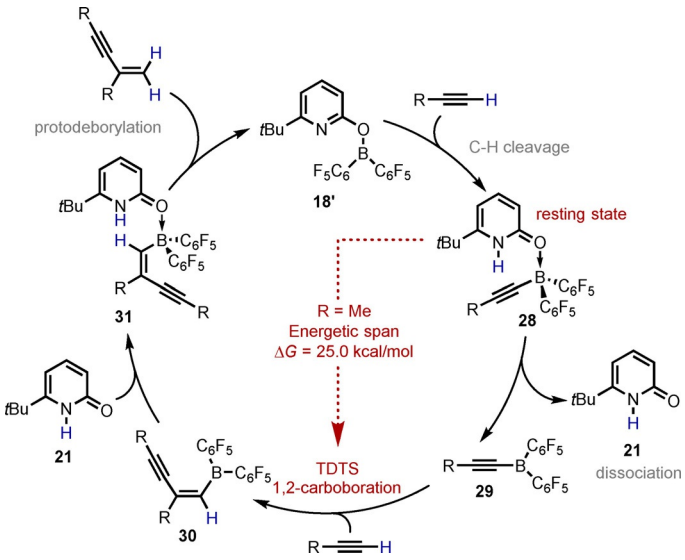

Scheme 16. Catalytic cycle of the *gem*-dimerization of terminal alkynes. The energetic span was computed at TightPNO-DLPNO-CCSD(T)/def2-TZVP//PBE0-D3(BJ)/def2-TZVP.[25,30] The SMD model for toluene was used to implicitly account for solvent effects.[26]

The 1,2-carboboration reaction was furthermore investigated by the reaction of the independently synthesized alkynylborane **32** with 3-phenylpropyne **33** (Scheme 17). The reaction yielded the enynylborane **34**, which was fully characterized by NMR spectroscopy. The addition of one equivalent of pyridone **21** yielded the enyne **35** and the bispyridone complex **23** as the protodeborylation product.

Computations showed that the 1,2-carboboration itself is concerted but highly asynchronous. The computed transition

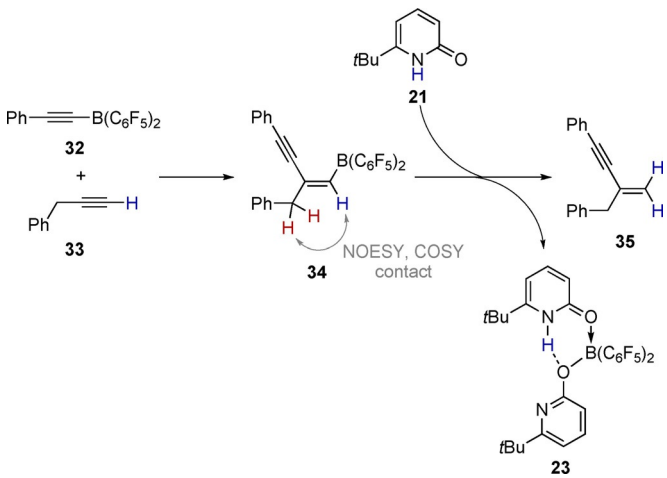

Scheme 17. 1,2-Carboboration of **33** by **32** and subsequent protodeborylation by the pyridone **21**.

state structure shows that the formation of the new C–B bond is more advanced than the formation of the new C–C bond (Figure 2).

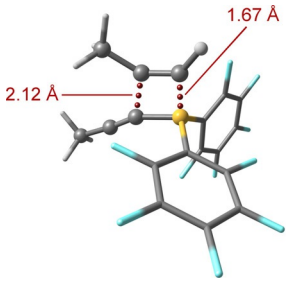

Figure 2. Computed transition state structure of the 1,2-carboboration with propyne as model substrate at PBE0(D3BJ)/def2-TZVP.[18]

Michael-addition of alkynylboranes to chalcones

Recently, Fountaine and co-workers reported the catalytic addition of *in situ* generated alkynylboranes to chalcones.[31] The active catalyst is formed by the transfer borylation of furanboronate **36** to the bifunctional mercaptoimidazole **37** (Scheme 18). The boronate moiety of **38** is transferred to a terminal alkyne (**39**), which changes the covalent N–B bond to a dative bond. This change to a dative bond enables the dissociation of the trivalent alkynylborane **40** and is thus essential for the observed reactivity. After dissociation, the free alkynylborane **40** adds to the chalcone[32] in a 1,4-addition, yielding the intermediary enolboronate **41**, which re-coordinates to imidazole **37**, yielding **42**. Protodeborylation liberates the product and regenerates the catalyst **38**. The scope was thoroughly investigated by using different alkynes and chalcone derivatives (Scheme 19). The authors demonstrated that this protocol can be transferred to different nitrogen- and sulfur-containing heterocycles as nucleophiles.

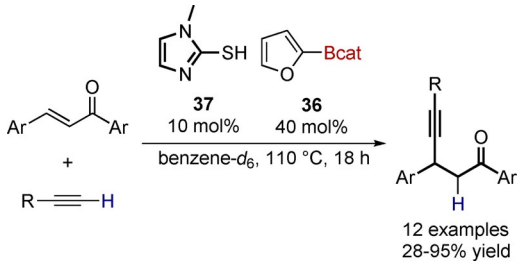

Scheme 19. Scope of the transfer borylation and the subsequent addition of alkynylboranes to chalcones.

Furthermore, potential deactivation pathways were investigated. By heating the catalyst **37** with trimethylsilylacetylene **43** and catecholboronate **36**, the formation of the boron-containing zwitterionic heterocycle **44**, which deactivates the catalyst, was observed (Scheme 20). The deactivation product is probably formed by thioboration of trimethylsilylacetylene by the *in situ* formed imidazole boronate **38**.

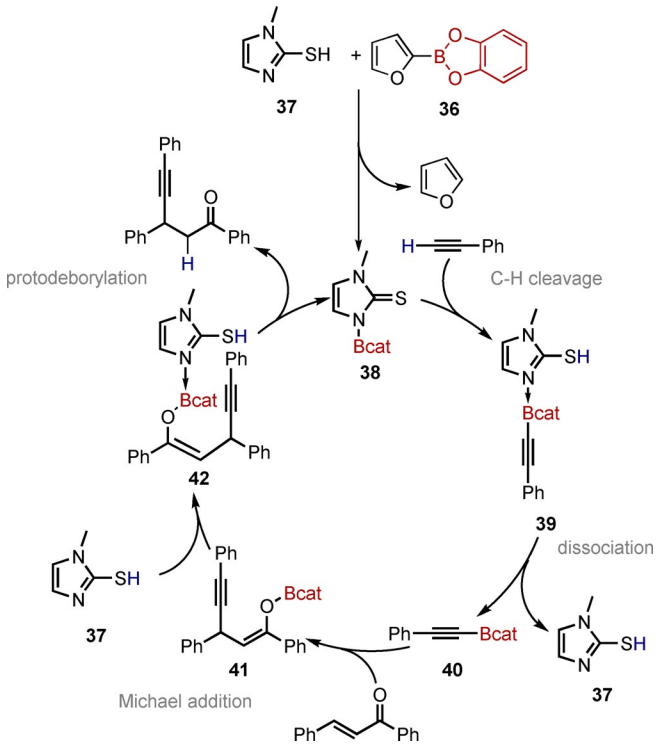

Scheme 18. Catalytic cycle of the transfer borylation, in situ formation of an alkynylborane and subsequent Michael addition to a chalcone.

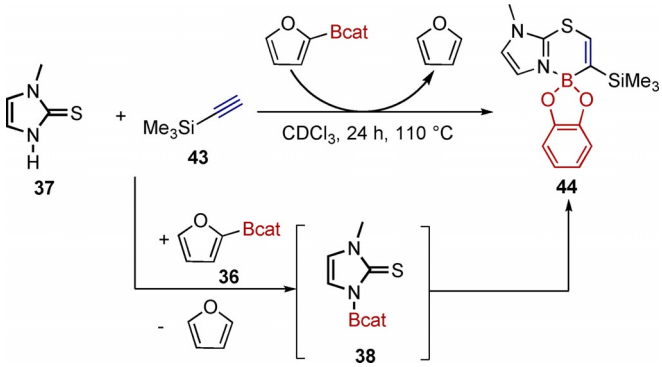

Scheme 20. Deactivation pathway of catalyst **37** by addition of trimethylsilylacetylene to imidazol boronate **38**.

Allylation of acetonitrile with in situ formed allylboranes

The allylation of electrophiles by allylboranes is an important and frequently used reaction in organic synthesis.[33,34] Brown and co-workers described the synthesis of such allylboranes by the hydroboration of allenes.[35] The approach for the synthesis of allylboranes by hydroboration of allenes in combination with BLC was used to realize a catalytic protocol for an allylation reaction requiring only catalytic amounts of an *in situ* formed allylation reagent (Scheme 21).[36] Hydrogen activation by the pyridonate borane **18′** forms the pyridone borane com-

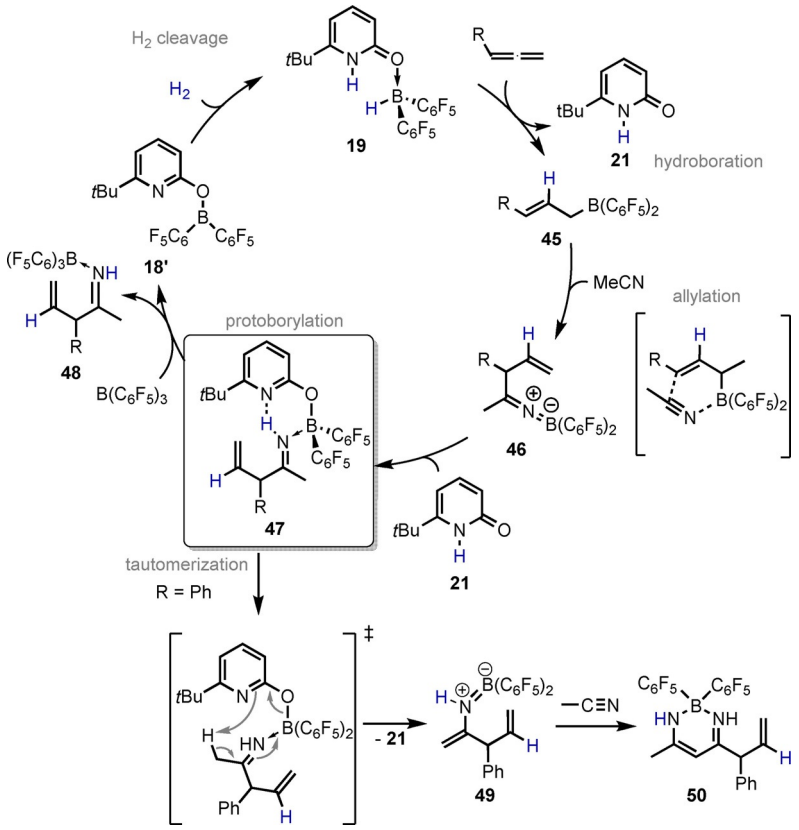

Scheme 21. Catalytic cycle of the allylation of nitriles by an in situ generated allylborane.

plex **19**, which dissociates into the pyridone **21** and Piers borane **22**. Adding an allene to the reaction mixture produces the allylborane **45**, which undergoes an allylation reaction with acetonitrile as electrophile yielding the ketiminoborane **46**. Re-coordination of the pyridone **21** to the ketiminoborane **46**, followed by a virtually barrierless proton transfer, affords complex **47** (gray rectangle in Scheme 21). This intermediate is critical for the outcome of the reaction because two different reaction paths can be observed. In the presence of $B(C_6F_5)_3$ (BCF) as an additional Lewis acid, the allylimine moiety of **47** can dissociate and form the kinetically stable complex **48** with BCF, while simultaneously catalyst **18′** is regenerated.

Without BCF, the pyridone moiety of **47** tautomerizes the allylimine to a nucleophilic enamineborane **49**, which dissociates and attacks a second equivalent of acetonitrile forming the β-diketiminate borane complex **50**. This prevents further catalytic reactivity because the $B(C_6F_5)_2$ moiety of catalyst **18′** is irreversible bound in **50**.

Both, the β-diketiminate borane **50** and the allylimine BCF complexes **48** are air- and moisture-stable and can be isolated by column chromatography in moderate to excellent yields (Scheme 22).

The formation of nucleophilic allylboranes from dihydrogen and allenes is a conceptually new way to use dihydrogen for organic synthesis.

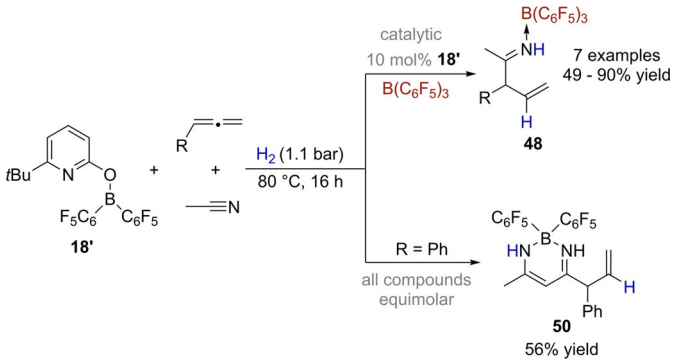

Scheme 22. Formation of the β-diketiminate borane **50** upon reaction of the pyridonate borane **18′** with an allene and acetonitrile under an H_2 atmosphere and the catalytic allylation of nitriles catalyzed by **18′** in the presence of BCF.

Transfer borylations

Fountaine and co-workers developed a catalytic protocol for the transfer borylation of 2-furylcatecholboran **36** to a wide range of heterocycles and terminal alkynes.[37,31] They developed two different types of catalysts (Scheme 23). The transfer borylation with the first catalyst—mercaptopyridine **51**—required relatively high catalyst loadings and five equivalents of the boron source catecholboronate **36** to borylate different N-, S-, and O-containing heterocycles.[37] The mercaptoimidazole **37** as the second catalyst generation was significantly more

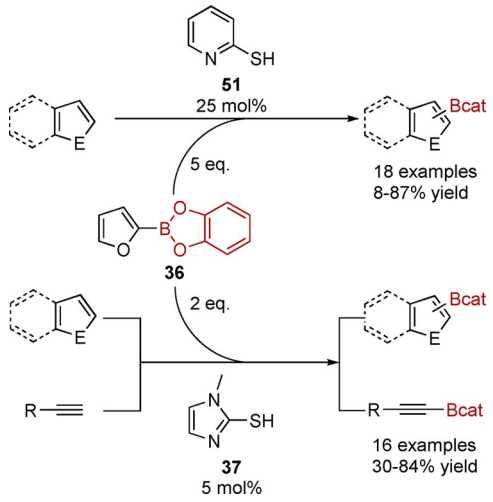

Scheme 23. Scope of the transfer borylation using **37** and **51**.

active.[31] The authors could show that they only needed 5 mol% catalyst loading to borylate the same heterocycles under milder conditions by using only two equivalents of catecholboronate **36**. Furthermore, by using **37** as the catalyst, they could expand the scope to terminal alkynes.

Both catalysts—mercaptopyridine **51** and mercaptoimidazole **37**—react through the same mechanism, which is in the following exemplified for **37** (Scheme 24). First, the nitrogen of the catalyst **37** coordinates to the catecholboronate, yielding **52**. In a protodeborylation, the boron moiety of the furan boronate **36** is transferred to the catalyst, yielding **38**. A concerted deprotonative borylation via $\mathbf{TS_{38/37}}$ transfers the boronate from the catalyst to the substrate. Here, the change from a covalent to dative N–B bond enables the dissociation of the product and regenerates the catalyst. This change of the bond mode can again be described as BLC.

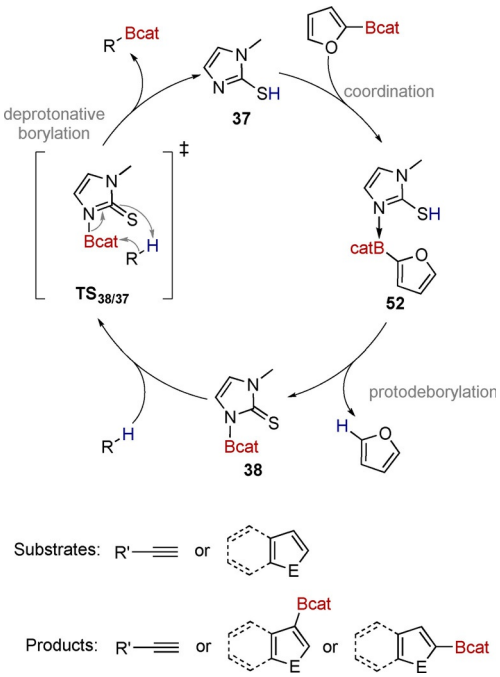

Scheme 24. Catalytic cycle of the transfer borylation.

Transfer hydrogenations with ammonia borane

Another example of BLC was presented in a series of publications on enantioselective transfer hydrogenations catalyzed by an FLP-type system by using ammonia borane as a hydrogen source. Du and co-workers showed that by using a catalytic amount of a chiral sulfinamide borane complex **53**, imines, indoles, enamines, and quinoxalines can be enantioselectively hydrogenated (Scheme 25).[38]

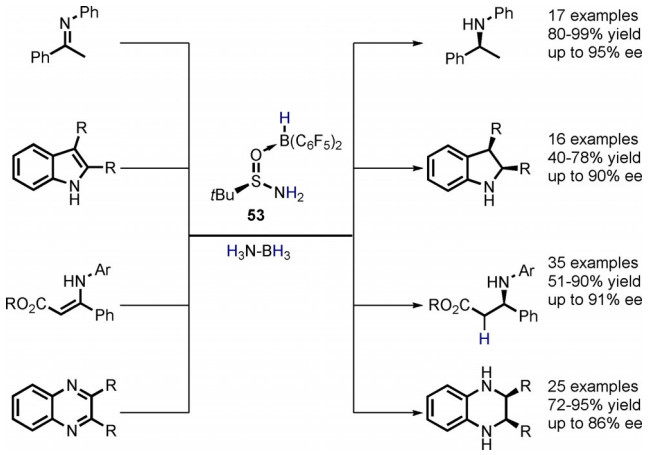

Scheme 25. Scope of the enantioselective transfer hydrogenation using **53** as the catalyst and ammonia borane as the hydrogen source.

Catalyst **53** is generated *in situ* by adding Piers borane **22** to the sulfinamide **54**. To assess the structure of the Lewis adduct formed in this way, the authors investigated the adduct formation of Piers borane **22** with all three Lewis basics sites of sulfinamide **54** computationally (Scheme 26). Based on these results, the authors concluded that the B–O coordinated form of **53** is the active catalyst.

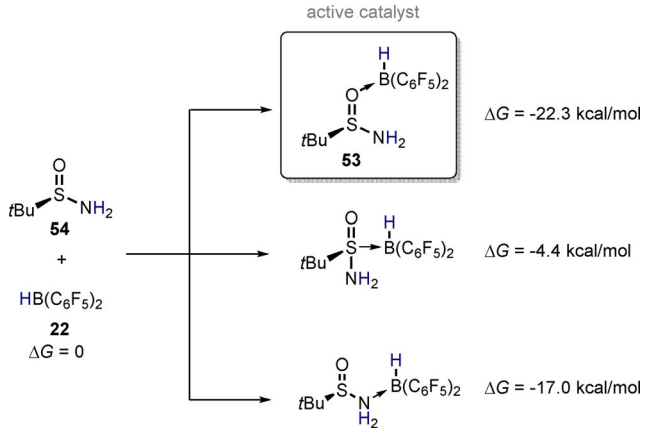

Scheme 26. Comparison of the different free complexation enthalpies of **54** and **22** computed at M06-2X/6-31G(d).[39] The PCM model for toluene was used to implicitly account for solvent effects.[40]

Mechanistic investigations revealed that the hydrogenation itself is a concerted transfer of the hydridic B–H and protic N–H of **53** to the respective substrate. However, according to DFT computations by the authors, the active species of the hydrogen transfer from the ammonia borane via $\mathbf{TS_{55/56}}$ is the sulfinamido borane **55** (Scheme 27). To regenerate the active catalyst **53**, the Piers borane moiety of **56** has to dissociate and recoordinate to the oxygen of the sulfinamide, which is only possible because of the change in bonding mode between boron and nitrogen in the course of the hydrogen transfer from the ammonia borane to **55**.

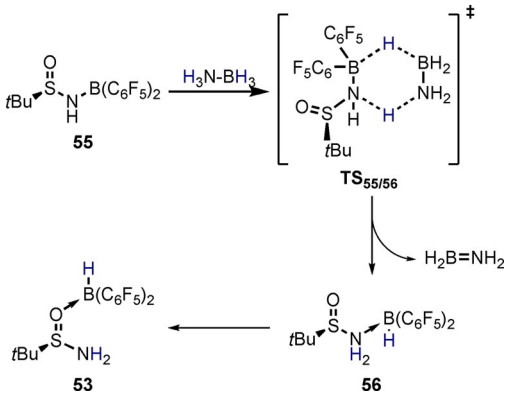

Scheme 27. Regeneration of the active catalyst **53** by hydrogen transfer from ammonia borane to sulfinamido borane **55**.

Summary and Outlook

We and others recently reported distinctive borane-based FLPs that can activate chemical bonds with a simultaneous change in the valence sphere of the borane. Specifically, the substituent at the borane that is involved in the bond activation becomes a datively bound ligand in a borane complex. To describe this mode of action, the term boron–ligand cooperation (BLC) was introduced. Within this Minireview, we provide criteria for BLC, framed in analogy to the criteria for MLC given by Khusnutdinova and Milstein. We furthermore discussed systems that fulfill these criteria. Although for some systems BLC is just a curiosity observed upon bond activation, certain systems provide access to the consequent reactivity, which can be used for novel catalytic reactions. Examples covered in this Minireview are hydroboration and 1,2-carboboration reactions or the metal-free transfer borylation for the synthesis of synthetically useful boronates. These reactivities rely on the presence of trivalent boranes formed upon dissociation of the respective borane complexes. As such a dissociation is not possible for classic intramolecular FLPs that form zwitterionic borates upon bond activation, BLC can complement the reactivity of classic FLPs. We hope that the discussion in this Minireview and the examples given stimulate the development of new metal-free catalysts.

Acknowledgments

This work was supported by the FCI (Liebig Fellowship to U.G.) and the DFG (Emmy-Noether program, GE 3117/1-1). Continuous support by Prof. Dr. P. R. Schreiner, Prof. Dr. R. Göttlich, and Prof. Dr. H. A. Wegner is acknowledged. Open access funding enabled and organized by Projekt DEAL.

Conflict of interest

The authors declare no conflict of interest.

Keywords: bond activation · boron–ligand cooperation · dissociation · frustrated Lewis pair · homogeneous catalysis

[1] a) R. Noyori, T. Ohkuma, *Angew. Chem. Int. Ed.* **2001**, *40*, 40–73; *Angew. Chem.* **2001**, *113*, 40–75; b) T. Ohkuma, H. Ooka, S. Hashiguchi, T. Ikariya, R. Noyori, *J. Am. Chem. Soc.* **1995**, *117*, 2675–2676; c) P. A. Dub, J. C. Gordon, *Nat. Rev. Chem.* **2018**, *2*, 396–408.
[2] a) J. Zhang, G. Leitus, Y. Ben-David, D. Milstein, *J. Am. Chem. Soc.* **2005**, *127*, 10840–10841; b) C. Gunanathan, D. Milstein, *Acc. Chem. Res.* **2011**, *44*, 588–602; c) D. Milstein, *Philos. T. R. Soc. A* **2015**, *373*, 20140189.
[3] J. R. Khusnutdinova, D. Milstein, *Angew. Chem. Int. Ed.* **2015**, *54*, 12236–12273; *Angew. Chem.* **2015**, *127*, 12406–12445.
[4] R. H. Crabtree, *The Organometallic Chemistry of the Transition Metals*, 4th ed., Wiley, New York, **2005**, pp. 32–35.
[5] For examples of bond activation by intramolecular boron-based FLPs, see: a) G. C. Welch, R. R. S. Juan, J. D. Masuda, D. W. Stephan, *Science* **2006**, *314*, 1124; b) P. Spies, G. Erker, G. Kehr, K. Bergander, R. Fröhlich, S. Grimme, D. W. Stephan, *Chem. Commun.* **2007**, 5072; c) Z. Jian, G. Kehr, C. G. Daniliuc, B. Wibbeling, G. Erker, *Dalton Trans.* **2017**, *46*, 11715; d) K. Chernichenko, M. Nieger, M. Leskelä, T. Repo, *Dalton Trans.* **2012**, *41*, 9029; e) K. Chernichenko, B. Kótai, I. Pápai, V. Zhivonitko, M. Nieger, M. Leskelä, T. Repo, *Angew. Chem. Int. Ed.* **2015**, *54*, 1749; *Angew. Chem.* **2015**, *127*, 1769; f) M.-A. Légaré, M.-A. Courtemanche, É. Rochette, F.-G. Fontaine, *Science* **2015**, *349*, 513; g) C. M. Mömming, E. Otten, G. Kehr, R. Fröhlich, S. Grimme, D. W. Stephan, G. Erker, *Angew. Chem. Int. Ed.* **2009**, *48*, 6643; *Angew. Chem.* **2009**, *121*, 6770; h) Z. Mo, E. L. Kolychev, A. Rit, J. Campos, H. Niu, S. Aldridge, *J. Am. Chem. Soc.* **2015**, *137*, 12227.
[6] For recent reviews about FLPs, see: a) J. Lam, K. M. Szkop, E. Mosaferi, D. W. Stephan, *Chem. Soc. Rev.* **2019**, *48*, 3592; b) D. W. Stephan, *J. Am. Chem. Soc.* **2015**, *137*, 10018; c) D. W. Stephan, *Org. Biomol. Chem.* **2012**, *10*, 5740; d) D. W. Stephan, *Science* **2016**, *354*, aaf7229; e) D. W. Stephan, G. Erker, *Chem. Sci.* **2014**, *5*, 2625; f) D. W. Stephan, G. Erker, *Angew. Chem. Int. Ed.* **2015**, *54*, 6400; *Angew. Chem.* **2015**, *127*, 6498; g) D. W. Stephan, S. Greenberg, T. W. Graham, P. Chase, J. J. Hastie, S. J. Geier, J. M. Farrell, C. C. Brown, Z. M. Heiden, G. C. Welch, M. Ullrich, *Inorg. Chem.* **2011**, *50*, 12338; h) J. Paradies, *Eur. J. Org. Chem.* **2019**, 283.
[7] a) L. Greb, F. Ebner, Y. Ginzburg, L. M. Sigmund, *Eur. J. Inorg. Chem.* **2020**, 3030; b) E. R. M. Habraken, A. R. Jupp, M. B. Brands, M. Nieger, A. W. Ehlers, J. C. Slootweg, *Eur. J. Inorg. Chem.* **2019**, 2436.
[8] E. Theuergarten, D. Schluns, J. Grunenberg, C. G. Daniliuc, P. G. Jones, M. Tamm, *Chem. Commun.* **2010**, *46*, 8561.
[9] E. Theuergarten, J. Schlösser, D. Schlüns, M. Freytag, C. G. Daniliuc, P. G. Jones, M. Tamm, *Dalton Trans.* **2012**, *41*, 9101.
[10] G. Lu, H. Li, L. Zhao, F. Huang, P. von R. Schleyer, Z.-X. Wang, *Chem. Eur. J.* **2011**, *17*, 2038.
[11] P. v. R. Schleyer, C. Maerker, A. Dransfeld, H. Jiao, N. J. R. van Eikema Hommes, *J. Am. Chem. Soc.* **1996**, *118*, 6317.
[12] U. Gellrich, Y. Diskin-Posner, L. J. W. Shimon, D. Milstein, *J. Am. Chem. Soc.* **2016**, *138*, 13307.
[13] U. Gellrich, *Angew. Chem. Int. Ed.* **2018**, *57*, 4779; *Angew. Chem.* **2018**, *130*, 4869.
[14] A. R. Katritzky, R. A. Jones, *J. Am. Chem. Soc.* **1960**, *82*, 2947.

[15] J. I. Wu, J. E. Jackson, P. von R. Schleyer, *J. Am. Chem. Soc.* **2014**, *136*, 13526.
[16] R. J. Gillespie, E. A. Robinson, *Angew. Chem. Int. Ed. Engl.* **1996**, *35*, 495; *Angew. Chem.* **1996**, *108*, 539.
[17] M. Ghara, S. Pan, P. K. Chattaraj, *Phys. Chem. Chem. Phys.* **2019**, *21*, 21267.
[18] a) J. P. Perdew, K. Burke, M. Ernzerhof, *Phys. Rev. Lett.* **1996**, *77*, 3865; b) C. Adamo, V. Barone, *J. Chem. Phys.* **1999**, *110*, 6158; c) S. Grimme, S. Ehrlich, L. Goerigk, *J. Comput. Chem.* **2011**, *32*, 1456; d) F. Weigend, R. Ahlrichs, *Phys. Chem. Chem. Phys.* **2005**, *7*, 3297.
[19] V. I. Minkin, *Pure Appl. Chem.* **1999**, *71*, 1919.
[20] F. Wech, M. Hasenbeck, U. Gellrich, *Chem. Eur. J.* **2020**, *26*, 13445.
[21] K. Chernichenko, Á. Madarász, I. Pápai, M. Nieger, M. Leskelä, T. Repo, *Nat. Chem.* **2013**, *5*, 718.
[22] For examples of alkyne hydrogenation with FLPs operating under a different mechanism, see: a) Y. Liu, L. Hu, H. Chen, H. Du, *Chem. Eur. J.* **2015**, *21*, 3495; b) K. C. Szeto, W. Sahyoun, N. Merle, J. L. Castelbou, N. Popoff, F. Lefebvre, J. Raynaud, C. Godard, C. Claver, L. Delevoye, R. M. Gauvin, M. Taoufik, *Catal. Sci. Technol.* **2016**, *6*, 882; c) J. L. Fiorio, N. López, L. M. Rossi, *ACS Catal.* **2017**, *7*, 2973; d) J. L. Fiorio, R. V. Gonçalves, E. Teixeira-Neto, M. A. Ortuño, N. López, L. M. Rossi, *ACS Catal.* **2018**, *8*, 3516-.
[23] T. Müller, M. Hasenbeck, J. Becker, U. Gellrich, *Eur. J. Org. Chem.* **2019**, 451.
[24] a) S. Kozuch, S. Shaik, *J. Am. Chem. Soc.* **2006**, *128*, 3355; b) S. Kozuch, S. Shaik, *Acc. Chem. Res.* **2011**, *44*, 101.
[25] a) G. Santra, N. Sylvetsky, J. M. L. Martin, *J. Phys. Chem. A* **2019**, *123*, 5129; b) E. Caldeweyher, C. Bannwarth, S. Grimme, *J. Chem. Phys.* **2017**, *147*, 034112; c) E. Caldeweyher, S. Ehlert, A. Hansen, H. Neugebauer, S. Spicher, C. Bannwarth, S. Grimme, *J. Chem. Phys.* **2019**, *150*, 154122; d) A. Hellweg, C. Hattig, S. Hofener, W. Klopper, *Theor. Chem. Acc.* **2007**, *117*, 587; e) F. Weigend, *J. Comput. Chem.* **2008**, *29*, 167; f) S. Grimme, J. G. Brandenburg, C. Bannwarth, A. Hansen, *J. Chem. Phys.* **2015**, *143*, 054107; g) H. Kruse, S. Grimme, *J. Chem. Phys.* **2012**, *136*, 154101; h) S. Grimme, J. Antony, S. Ehrlich, H. Krieg, *J. Chem. Phys.* **2010**, *132*, 154104; i) F. Weigend, *Phys. Chem. Chem. Phys.* **2006**, *8*, 1057.
[26] A. V. Marenich, C. J. Cramer, D. G. Truhlar, *J. Phys. Chem. B* **2009**, *113*, 6378.
[27] For examples of reactions of borane-based FLPs with terminal alkynes, see: a) M. A. Dureen, C. C. Brown, D. W. Stephan, *Organometallics* **2010**, *29*, 6594; b) M. A. Dureen, D. W. Stephan, *J. Am. Chem. Soc.* **2009**, *131*, 8396; c) C. Jiang, O. Blacque, H. Berke, *Organometallics* **2010**, *29*, 125; d) C. M. Mömming, G. Kehr, B. Wibbeling, R. Fröhlich, B. Schirmer, S. Grimme, G. Erker, *Angew. Chem. Int. Ed.* **2010**, *49*, 2414; *Angew. Chem.* **2010**, *122*, 2464; e) T. Voss, T. Mahdi, E. Otten, R. Fröhlich, G. Kehr, D. W. Stephan, G. Erker, *Organometallics* **2012**, *31*, 2367.
[28] M. Hasenbeck, T. Müller, U. Gellrich, *Catal. Sci. Technol.* **2019**, *9*, 2438.
[29] For different examples of 1,2-carboboration reactions, see: a) M. Devillard, R. Brousses, K. Miqueu, G. Bouhadir, D. Bourissou, *Angew. Chem. Int. Ed.* **2015**, *54*, 5722; *Angew. Chem.* **2015**, *127*, 5814; b) I. A. Cade, M. J. Ingleson, *Chem. Eur. J.* **2014**, *20*, 12874; c) Y. Shoji, N. Tanaka, S. Muranaka, N. Shigeno, H. Sugiyama, K. Takenouchi, F. Hajjaj, T. Fukushima, *Nat. Commun.* **2016**, *7*, 12704; d) M. F. Lappert, B. Prokai, *J. Organomet. Chem.* **1964**, *1*, 384; e) Y. Cheng, C. Mück-Lichtenfeld, A. Studer, *J. Am. Chem. Soc.* **2018**, *140*, 6221.
[30] a) C. Riplinger, B. Sandhoefer, A. Hansen, F. Neese, *J. Chem. Phys.* **2013**, *139*, 134101; b) F. Neese, *WIREs Comput. Mol. Sci.* **2012**, *2*, 73.
[31] V. Desrosiers, C. Z. Garcia, F.-G. Fontaine, *ACS Catal.* **2020**, *10*, 11046.
[32] T. R. Wu, J. M. Chong, *J. Am. Chem. Soc.* **2005**, *127*, 3244.
[33] W. R. Roush, *Comprehensive Organic Synthesis, Vol. 2* (Eds.: B. M. Trost, I. Fleming), Pergamon, New York, **1991**, pp. 1 – 53.
[34] a) H. C. Brown, P. K. Jadhav, *J. Am. Chem. Soc.* **1983**, *105*, 2092; b) H. C. Brown, K. S. Bhat, *J. Am. Chem. Soc.* **1986**, *108*, 5919; c) U. S. Racherla, H. C. Brown, *J. Org. Chem.* **1991**, *56*, 401; d) W. R. Roush, A. D. Palkowitz, K. Ando, *J. Am. Chem. Soc.* **1990**, *112*, 6348.
[35] G. W. Kramer, H. C. Brown, *J. Organomet. Chem.* **1977**, *132*, 9.
[36] M. Hasenbeck, S. Ahles, A. Averdunk, J. Becker, U. Gellrich, *Angew. Chem. Int. Ed.* **2020**, *59*, 23885; *Angew. Chem.* **2020**, *132*, 24095.
[37] É. Rochette, V. Desrosiers, Y. Soltani, F.-G. Fontaine, *J. Am. Chem. Soc.* **2019**, *141*, 12305.
[38] a) W. Zhao, Z. Zhang, X. Feng, J. Yang, H. Du, *Org. Lett.* **2020**, *22*, 5850; b) S. Li, W. Meng, H. Du, *Org. Lett.* **2017**, *19*, 2604; c) S. Li, G. Li, W. Meng, H. Du, *J. Am. Chem. Soc.* **2016**, *138*, 12956; d) W. Zhao, X. Feng, J. Yang, H. Du, *Tetrahedron Lett.* **2019**, *60*, 1193.
[39] a) Y. Zhao, D. G. Truhlar, *Acc. Chem. Res.* **2008**, *41*, 157; b) Y. Zhao, D. G. Truhlar, *Theor. Chem. Acc.* **2008**, *120*, 215; c) R. Ditchfield, W. J. Hehre, J. A. Pople, *J. Chem. Phys.* **1971**, *54*, 724; d) W. J. Hehre, R. Ditchfield, J. A. Pople, *J. Chem. Phys.* **1972**, *56*, 2257.
[40] G. Scalmani, M. J. Frisch, *J. Chem. Phys.* **2010**, *132*, 114110.

Manuscript received: October 13, 2020
Revised manuscript received: December 2, 2020
Accepted manuscript online: December 9, 2020
Version of record online: January 28, 2021

